CARBON 49 (2011) 1919–1930

available at www.sciencedirect.com

ScienceDirect

journal homepage: www.elsevier.com/locate/carbon

Effect of functionalization on the thermo-mechanical and electrical behavior of multi-wall carbon nanotube/epoxy composites

L. Guadagno [a,d,*], *B. De Vivo* [b,d], *A. Di Bartolomeo* [c,d], *P. Lamberti* [b,d], *A. Sorrentino* [a], *V. Tucci* [b,d], *L. Vertuccio* [a,d], *V. Vittoria* [a,d]

[a] *Dipartimento di Ingegneria Chimica e Alimentare, Università di Salerno, Via Ponte Don Melillo, 84084 Fisciano (SA), Italy*
[b] *Dipartimento di Ingegneria dell'Informazione e Ingegneria Elettrica, Università di Salerno, Via Ponte Don Melillo, 84084 Fisciano (SA), Italy*
[c] *Dipartimento di Fisica "E. Caianiello", Via S Allende, 84081 Baronissi (SA), Italy*
[d] *Nano-Mates, Research Centre for NANOMAterials and nanoTEchnology, Università di Salerno, Via S. Allende, 84081 Baronissi (SA), Italy*

ARTICLE INFO

Article history:
Received 13 August 2010
Accepted 10 January 2011
Available online 12 January 2011

ABSTRACT

The effect of the functionalization of multi-wall carbon nanotubes (MWCNTs) on the structure, the mechanical and electrical properties of composites was investigated. Samples based on epoxy resin with different weight percentage of MWCNTs or COOH-functionalized carbon nanotubes (MWCNT–COOH) were prepared and characterized. Dynamic-mechanical thermal analysis shows that the storage modulus increases with the addition of MWCNTs, whereas a constant value or even a weak reduction was observed for functionalized nanotubes. Two phases were suggested in the composites with MWCNT–COOH, both by dynamic-mechanical properties and by water transport. Chemical functionalization of MWCNTs increases the compatibility with the epoxy matrix due to the formation of an interface with stronger interconnections. This, in turn, causes a significant decrease in the electrical conductivity of this type of composite with respect to the untreated MWCNTs which can be explained in terms of tunnelling resistance between interacting nanotubes.

1. Introduction

The increased demand for high-quality multifunctional materials in different industrial applications is the driving force of the huge research effort dedicated to the formulation and preparation of advanced nanostructured composites with superior characteristics. In particular, a suitable design of the multifunctional composites can be achieved by choosing the appropriate synthetic polymers and fillers as well as the incorporation methods tailored to optimize the polymer-filler interface.

Among thermosetting polymers, epoxy-based systems, due to their excellent mechanical properties for structural stability, allow to manufacture a very versatile class of composites for structural applications in automotive, aeronautics, marine industry, electronics and others.

When used as fillers carbon nanotubes (CNTs) for their distinctive structural and transport properties, such as excellent strength, modulus, electrical and thermal conductivities along with low density, enable the fabrication of composites with unmatched multi-functional characteristics [1–3]. The achievable range of the composite properties can be very large since CNTs with different forms, geometries and functionalities can be exploited. In fact, depending on preparation method and processing conditions single wall (SW), double wall (DW) or multi wall (MW) CNTs of various length,

---

[*] *Corresponding author*: Fax: +39 089 964057.
E-mail address: lguadagno@unisa.it (L. Guadagno).

0008-6223/$ - see front matter © 2011 Elsevier Ltd. All rights reserved.
doi:10.1016/j.carbon.2011.01.017

diameters (and hence aspect ratio) and chirality can be incorporated, whereas suitable chemical or physical treatments may lead to different surface morphologies, which, in turn, may improve their dispersion and adhesion in the polymeric matrix [4–5].

In particular, epoxy-based composites with very low concentrations of MWCNTs, preserving the remarkable mechanical properties and surface finish properties of the matrix and exhibiting a sufficiently high electrical conductivity (greater than 10^{-6} S/m) have been proposed for the dissipation of electrostatic charges, for electromagnetic shielding, electronic packaging, sensors and as structural parts in automotive and aerospace applications [6–9]. However much higher conductivities are required in several applications, as for example in aerospace applications, if the lightning strike problem has to be solved for epoxy resins to fully replace the metallic parts of the aircrafts.

The most relevant issues to be considered in the development of innovative CNT-based composites with improved mechanical and electrical properties are: (i) the possibility to achieve an effective dispersion of CNTs (ii) the capability to create a strong adhesion to the polymeric matrix leading to the formation of strong interfacial bonding. The two effects are not strictly related, because one can have a good dispersion without achieving strong adhesion; moreover the second effect, determinant for mechanical properties, is less important for electrical conductivity. An optimization of the composite may be pursued by varying the CNT type, preparation technique and processing parameters. Although several research groups have analyzed these relevant issues by considering either the basic physical phenomena or the technological aspects, there are still different questions to clarify [5,10–16]. For example the oxidation of CNT performed to create a more homogeneous dispersion into the polymer, can induce nanotube damage considerably affecting both mechanical and electrical properties and depending on the oxidative treatment [14,16].

Recent reviews considering most of the published results on this topic pointed out some interesting results, regarding the maximum achievable conductivity. Interestingly, type (SWCNT or MWCNT) and treatment (purification and oxidation) of the nanotubes do not show a clear impact on the maximum conductivity, whereas contradicting results about the dependence of the conductivity on the aspect ratio are reported. Indeed, dispersion seems the determinant factor to reach higher conductivity. As an example, it was reported that the epoxy composites filled with well dispersed CNTs yield much higher values of electrical and thermal conductivity than samples with poor dispersion [5]. It is suggested that this happens because the well dispersed CNTs can effectively form conductive paths even at lower loading. However, we emphasize that the best dispersion not necessarily leads to the highest conductivities, since a good dispersion can imply the formation of a polymer layer around the carbon nanotubes, which encapsulate and insulate it, thus preventing the formation of a high-conductance percolation path.

Therefore, further investigations on these issues are needed to enrich basic knowledge and achieve efficient material design.

For these reasons, we have considered a variety of methods of incorporation in an epoxy matrix formed by Diglycidyl ether of bisphenol A (DGEBA) cured with 4,4′-diaminodiphenyl sulfone (DDS) of several types of CNTs (single, double, multi walled and organically modified). The study was aimed at correlating the structural organization of the composites, depending on nanotube type, with physical and electrical properties. The effects of different dispersion methods and cure parameters has been discussed in a previous paper [17]. In this work, the mechanical and electrical properties of the epoxy systems in presence of increasing concentrations of multi-walled and chemically functionalized carbon nanotubes are discussed to enlighten the effect of functionalization, with reference to the morphological characteristics of the composites. The presence of –COOH chemical groups on the MWCNT is expected to improve the dispersion into the matrix and therefore can help understanding how this factor influences the physical, and in particular the electrical, properties. We show that the nanotube functionalization with –COOH has a strong influence on the electrical properties and results in a remarkable reduction of the conductance of the composite.

2. Materials and methods

The composites are manufactured by using as base epoxy resin DiGlycidil-Ether Bisphenol-A (DGEBA), with 4,4′-diaminodiphenyl sulfone (DDS), as hardener agent. The MWCNTs (3100 Grade) and MWCNT–COOH (3101 Grade) were obtained from Nanocyl S.A. The specific surface area of both multi-wall carbon nanotubes determined with the BET method is around 250–300 m^2/g, the carbon purity is >95% with a metal oxide impurity <5% as it results by thermogravimetric analysis (TGA).

Epoxy and DDS were mixed at 120 °C and the MWCNTs were added and incorporated into the matrix by using a ultrasonication for 20 min (Hielscher model UP200S-24 KHz high power ultrasonic probe). Such an incorporation method has been chosen among other different techniques since it leads to the composites characterized by the best mechanical and electrical properties [18]. All the mixtures were cured at 150 °C for 1 h and 220 °C for 3 h. In this paper composites with MWCNTs and functionalized MWCNT–COOH are named ENX and EFX, respectively, where X represents the CNT percentage. As example EN0.5 is the Epoxy resin filled with non functionalized carbon nanotubes at 0.5% concentration w/w%.

The transmission electron microscopy (TEM) characterization was performed on a JEOL 2010 LaB_6 microscope operating at 200 kV. Nanopowder was dispersed (in ethanol) by ultrasonic waves for 30 min. The obtained suspension was dropped on a copper grid (Holey carbon).

High resolution scanning electron microscope (HRSEM) micrographs were obtained with a field emission SEM apparatus (JSM-6700F, JEOL) instrument operating at 3 kV.

Some of the composite sections were cut from the solid samples by a sledge microtome. These slices were etched before the observation by SEM microscopy. The etching reagent was prepared by stirring 1.0 g potassium permanganate in a solution mixture of 95 ml sulfuric acid (95–97%) and 48 ml orthophosphoric acid (85%). The films were immersed into the fresh etching reagent at room temperature and held under agitation for 24 h. Subsequent washings were done using a cold mixture of two parts by volume of concentrated sulpfuric acid and seven parts of water. Afterwards the samples were washed again with 30% aqueous hydrogen peroxide to remove any manganese dioxide. The samples were finally washed with distilled water and kept under vacuum for 2 days.

The Raman spectra were collected at room temperature with a microRaman spectrometer Renishaw inVia operating with a 514-nm laser source.

Thermal analysis was performed with a Mettler DSC 822 differential thermal analyzer in a flowing nitrogen atmosphere. The curing reaction of the resins with and without MWCNTs was performed in dynamic regime, by heating in the Differential Scanning Calorimeter (DSC) at 10 °C/min from 0 to 350 °C.

The infrared spectra were obtained in absorbance by using a FTIR-Bruker Vertex 70 spectrophotometer with a resolution of 4 cm^{-1} (32 scans collected).

Dynamic-mechanical properties of the samples were performed with a dynamic mechanical thermo-analyzer (TA instrument-DMA 2980). Solid samples with dimensions $4 \times 10 \times 35$ mm were tested by applying a variable flexural deformation in dual cantilever mode. The displacement amplitude was set to 0.1%, whereas the measurements were performed at the frequency of 1 Hz. The range of temperature was from −60 °C to 300 °C at the scanning rate of 3 °C/min.

The measurements of the dc volume conductivity were performed by using disk-shaped specimens of about 2 mm thickness and 10–50 mm diameter. Surface leakage currents were found to be negligible with respect to volume current, whence no guard ring was used. The measurement system, remotely controlled by the software LABVIEW®, is composed of a voltage generator FUG HCN 35-6500 (max output current 5 mA), a pico-ammeter Keithley 6514 (min current 10^{-13} A), and a suitable shielded cell with temperature control. The max value of applied electric field is limited to 1.0 kV/m in order to avoid Joule heating of samples.

3. Results and discussion

3.1. *Carbon nanotube characterization*

3.1.1. *Morphological analysis*

In Figs. 1a and 1b, HR-TEM images of the pristine MWCNTs and MWCNT–COOH are reported.

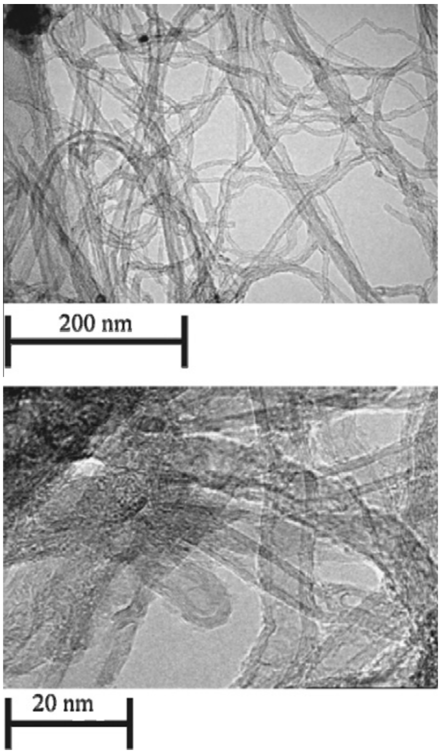

Fig. 1a – High resolution transmission electron microscope images of MWCNTs.

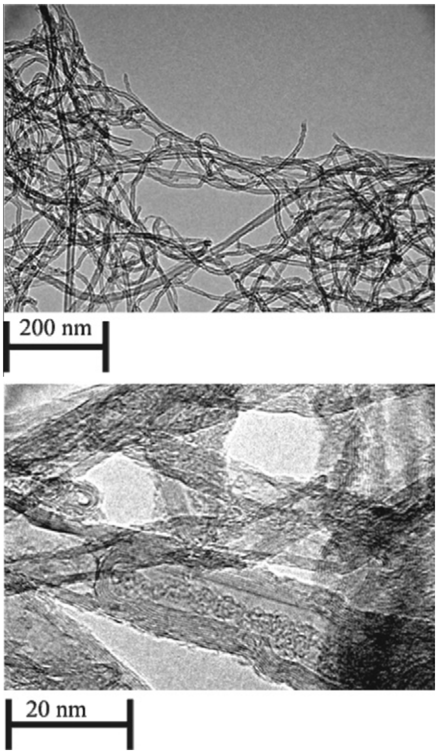

Fig. 1b – High resolution transmission electron microscope images of MWCNT-COOH.

MWCNTs are characterized by an outer diameter ranging from 10 to 30 nm. CNT length is from hundreds of nm to some micrometer. Number of walls varies from 4 to 20 in most nanotubes. It is worth noting that multi-wall carbon nanotubes functionalized with COOH (Fig. 1b) were prepared from the same batch of MWCNTs, so that the mean aspect ratio is the same, assuming that the functionalization procedure did not influence it, as reported by the technical report of Nanocyl. The samples are produced via the catalytic carbon vapor deposition (ccvd) process. Nanotubes which exit the reactor are then purified to greater than 95% carbon to produce the 3100 grade. This grade is then functionalized with COOH to produce the 3101 grade. The value of unit (%) of COOH functionalization, measured by XPS method, is about four. As shown in Figs. 1a and 1b, CNTs appear to be reasonably well separated in both cases.

3.1.2. *Raman spectroscopy*

Raman spectroscopy of CNTs provides information on the degree of structural ordering and therefore the bonding states of carbons in the nanotube structure. The Raman spectra collected for MWCNTs and MWCNT–COOH are shown in Fig. 2.

The Raman spectra are similar in shape; they exhibit two strong bands, the D mode (1350 cm^{-1}) and the tangential stretching G mode (1586 cm^{-1}) and two weak bands, the G′-band (overtone of D mode) at 2700 cm^{-1} and the 2LO band (overtone of LO mode) at 2900 cm^{-1}.

The D-band is a double-resonance Raman mode affected by defects in the graphene structure. This band together with the G′-band can be used for material characterization to probe and monitor structural modifications of the nanotube sidewalls that come from the introduction of defects and the attachment of different chemical specie [18]. The G-band consists of two components that are generally distinguishable in the spectrum of SWCNTs with a peak at 1590 cm^{-1} (G^+) and another at about 1570 cm^{-1} (G^-). The G^+ feature is associated with carbon atom vibrations along the nanotube axis (LO phonon mode). The G^- feature, in contrast, is associated with vibrations of carbon atoms along the circumferential direction of the SWCNTs. In our spectra, as already reported by other authors [18], we observe a single peak for the G-band because the $G^+ - G^-$ splitting in MWCNTs is both small in intensity and smeared out by the effect of the diameter distribution within the individual MWCNTs, and the ensemble of MWCNTs. In our spectra the G-band feature only exhibits a weakly asymmetric characteristic lineshape, with a peak appearing close to the graphite frequency (1582 cm^{-1}).

The intensity and characteristics of this band give information on the order of graphitic layers in the carbon nanostructured forms [19–21]. In particular, a high ratio R of intensities of the D and G bands ($R = I_D/I_G$) indicates a high quantity of structural defects.

The R values of our CNTs are 1.19 for MWCNTs and 1.30 (i.e. 10% higher) for MWCNT–COOH. This small percentage increase of the R value is expected not to affect the properties of composites.

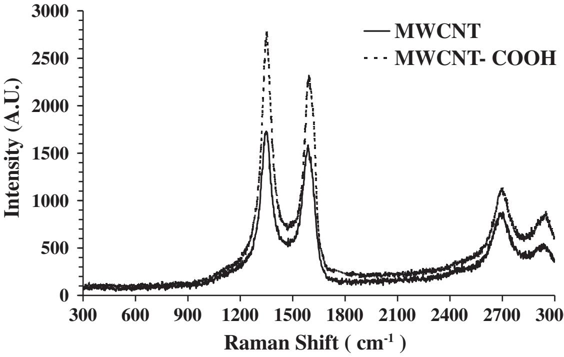

Fig. 2 – Raman spectra of MWCNTs and MWCNT–COOH.

3.2. *Composite characterization*

3.2.1. *Cure behavior*

To investigate the differences between the two kinds of tubes incorporated into the resin, we studied the cure behavior in dynamic regime. In Fig. 3 we show the differential scanning calorimetric (DSC) curves increasing the temperature between 0 °C and 300 °C for samples with MWCNTs (a) and with MWCNT–COOH (b) at different concentrations.

Both series show a principal peak centered at about the same temperature of the neat resin, and a small peak at higher temperature, which is also present in the neat resin. However in the samples with MWCNTs the small peak decreases in intensity and shifts leftwards with increased nanotube concentration, and disappears for 1% MWCNT concentration; for samples with MWCNT–COOH, the peak has the same shift in temperature but maintains and even increases its intensity while increasing the concentration.

To emphasize this effect we show in Fig. 4 the curves for samples with the highest concentration of MWCNTs and MWCNT–COOH.

The small peak can be associated to a small fraction of resin homo-polymerization, whose temperature is reduced by the presence of the non functionalized MWCNT nanotubes, whereas the –COOH function also increases the fraction of homopolymer, probably as consequence of the interaction of the functional group with the epoxy group. Another possibility is an esterification reaction between the –COOH and the epoxy not completely reacted, also determining a small fraction of a different phase. The possible presence of two phases

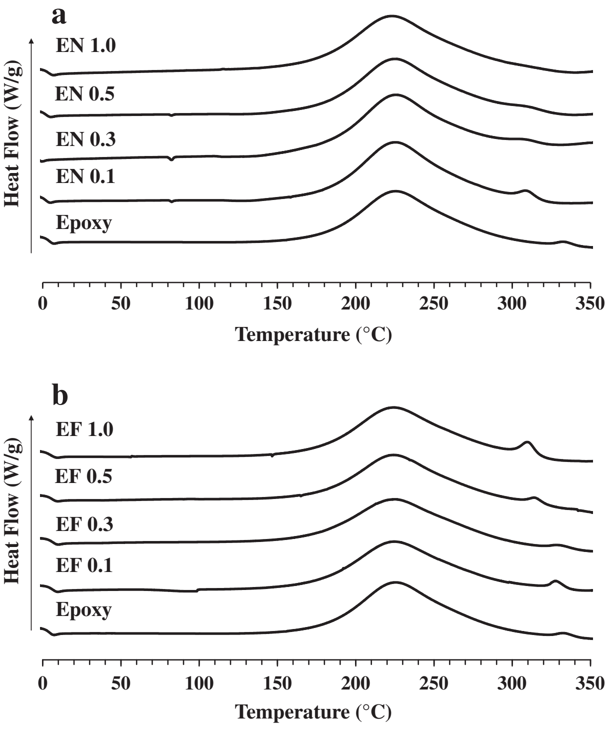

Fig. 3 – DSC heating curves for the two epoxy resins with different percentage of MWCNTs (a) and of MWCNT–COOH (b).

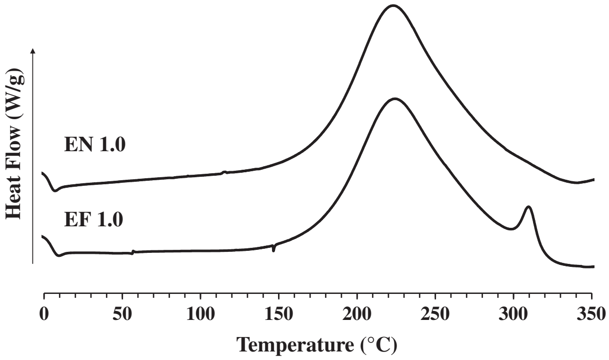

Fig. 4 – DSC heating curves for the two epoxy resins with 1% of the different carbon nanotubes.

in the MWCNT–COOH samples, confirmed in the following characterization, is anticipated by observing the DSC curves for the cure reaction.

3.2.2. *FTIR analysis*

The FTIR spectral analysis of the resins cured with MWCNT and MWCNT–COOH was performed to verify possible structural differences in the two series of samples. The analysis is based either on the appearance of different bands or on the intensity change of functional groups. According to the previous DSC results we may suggest the formation of a small fraction of homopolymer in samples filled with –COOH functionalized nanotubes. If this is the case, we ought to observe a difference in the ether region, since the homo-polymerization is based on an ether link formation. The characteristic response of ethers in the IR is associated with the stretching vibration of the C–O–C system [22]. However, since the vibrational characteristics of this system does not differ greatly from C–C–C system, the response to C–O–C stretching can be found in the same region, determining an overlapping of bands. Moreover the vibrational bands of the aryl alkyl ethers (aryl–O–CH_2–), due to the structure of the epoxy resin precursor, are already present in the FTIR spectra, in the interval in which the aliphatic ethers appear. It is therefore very difficult to put in evidence a small contribution of the aliphatic ether band into the spectra. At variance we can base the analysis on the –OH band, considering that in the homo-polymerization less –OH groups are formed with respect to the cross-linking reaction (see supporting information).

In Fig. 5 we show the FTIR spectra in absorbance between 500 and 4000 cm^{-1}, for the samples with 1% of MWCNT, 1% of MWCNT–COOH and 4% of MWCNT–COOH. The –OH bands appear around 3400 cm^{-1}, and their intensity was normalized with the intensity of the band at 1593 cm^{-1}, due to the aromatic C=C stretching.

In Table 1 we report the value of the ratio $R = \frac{A(3408)}{A(1593)}$ calculated for the three samples.

We observe a lower value of R for the samples filled with functionalized carbon nanotubes. In particular the sample with 1% of MWCNT–COOH shows a value 14% lower and the sample with 4% of MWCNT–COOH a value 20% lower than the sample with un-functionalized CNT. This is in good agreement with the suggestion of a small fraction of homo-polymerization, induced by the functionalized carbon nanotubes.

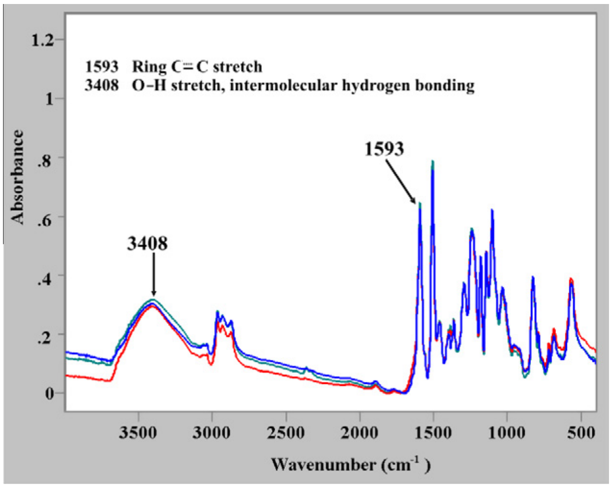

Fig. 5 – FTIR spectra of EN 1.0 (red spectrum), EF 1.0 (green spectrum), EF 4.0 (blue spectrum) samples. (For interpretation of the references to color in this figure legend, the reader is referred to the web version of this article.)

Table 1 – Absorbance ratio R of EN 1.0, EF 1.0, EF 4.0 samples.

Sample	$R = \frac{A(3408)}{A(1593)}$
EN 1.0	0.393
EF 1.0	0.340
EF 4.0	0.313

3.2.3. *Morphological analysis*

In order to analyze the homogeneity of the nanofiller dispersion in the polymeric matrix, the samples with MWCNT and with MWCNT–COOH at 0.5 w% were investigated by means of scanning electron microscopy (SEM). In Figs. 6a and 6b we show different zones of the fracture surface of the two different composites. The analysis was carried out on etched samples to remove the resin surrounding the nanotubes, leaving them bare. The used etching procedure, reported in the experimental, mainly consumes the surface layers of the polymeric matrix. We observe that the same etching procedure seems to be more efficient for composites filled with un-functionalized MWCNTs. In fact, in this case we observe whole lengths of the carbon nanotube segments released from the residual resin fraction. Instead, composites with MWCNT–COOH do not show bare nanotubes: this can be explained assuming that strong interconnections between nanotubes and residual polymeric matrix remain after the etching attack. A careful observation also highlights for both the samples with MWCNTs and with MWCNT–COOH a homogeneous structure in which the CNTs are uniformly distributed in a close net through the epoxy matrix.

3.2.4. *Mechanical properties*

The storage modulus, E' (MPa), and the loss factor, tanδ, of the neat epoxy and the composites with different MWCNT concentrations are shown in Fig. 7a and b.

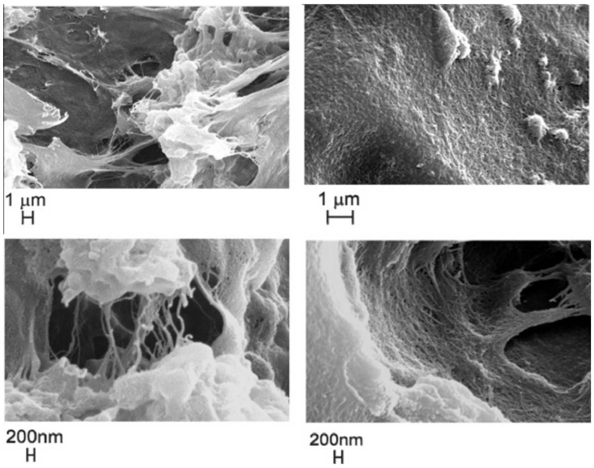

Fig. 6a – SEM images of the fracture surface of the two different composites with 0.5 wt% loading of CNTs (left: MWCNTs and right: MWCNT–COOH).

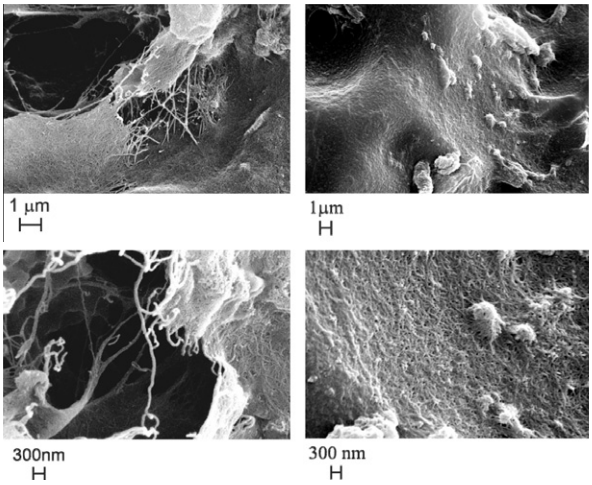

Fig. 6b – SEM images of the fracture surface of the two different composites with 0.5 wt% loading of CNTs (left: MWCNTs and right: MWCNT–COOH).

At low temperatures all the samples show a very high value of the elastic modulus, followed by two little drops due to second order transitions between −20 and 0 °C the first and between 50 °C and 70 °C the second. The principal drop, due to the glass transition, is evident for all samples in the range 220–240 °C. In this temperature range also the tanδ curves show a peak indicating the glass transition temperature of the material. All the samples present almost identical peak height and position in the loss factor curves. This indeed means that the MWCNT, at the investigated concentrations, have no particular effect on the relaxation phenomena leading to the glass transition of the system. As far as the storage modulus is concerned it shows a slight increase with the MWCNT concentration. In particular, at high temperatures, the addition of 1.0% in mass (corresponding to about 0.6% in volume) of carbon nanotubes shows an improvement of the storage modulus up to 20% in the temperature range between 70 and 150 °C. However the CNT reinforcing effect of 20% is less than expected. Indeed there are many factors that influence the overall mechanical properties of CNT-reinforced composites; among these, the weak bonding between CNTs and matrix, curviness and agglomeration of CNTs, and structural parameters as aspect ratios, diameters, wall numbers, etc. To deeply understand the influence of CNTs on the mechanical properties of the material, it would be necessary to factorize the contributions of all these parameters considering a massive lot of experiments. Undeniably, our results, and also others reported in literature, show that the CNT-reinforced composites do not reach optimum results; the improvement is even much less than expected from a simple mixing rule. In our experience the reinforcement role of CNTs (although below the theoretical value) can be very different and strongly dependent on the chemical nature of the epoxy matrix; this is related to the chemical nature of the epoxy precursor and hardener, their stoichiometric ratios and curing conditions. A sound choice of the matrix components allows to modulate, within limits, the matrix stiffness.

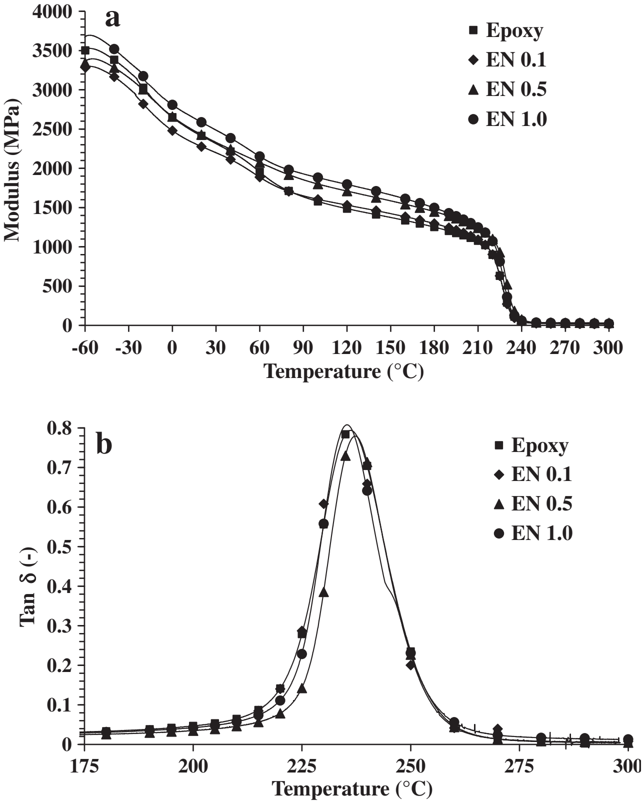

Fig. 7 – (a) Storage modulus, E′ (MPa) and (b) loss factor (tanδ) of the pure epoxy and its composites with different MWCNTs concentrations.

About the nanofiller role, by introducing high strength, high modulus nanotubes into a low strength, low modulus matrix, an increase of the composite strength is to be expected because load is transferred to the high strength tubes. The effectiveness of the load transfer depends on the difference in moduli between the nanotubes and the matrix. Indeed, we have always found that the reinforcement role of MWCNTs decreases with increasing the stiffness matrix. By way of example, we can report the results of our previous paper [22] where the influence of the same MWCNTs was analyzed on an epoxy matrix cured with a tertiary amine as a catalyst for the curing reactions. The analyzed composites, as expected, showed lower values of the elastic modulus with respect to the composites cured with DDS discussed here. In the case of the composites cured with a tertiary amine, the storage modulus of the filled composite (1% of MWCNTs) is ~200 % higher than the unfilled resin. These observations are in agreement with other results reported in literature that show a reinforcement role of CNTs for epoxy precursor cured with hardener that produce less rigid matrixes [23,24]. To clarify this aspect, a very pertinent work was done by Her and Yeh [25]. They have carried out a systematic investigation on the effect of the matrix stiffness and content of multi-walled carbon nanotubes on the mechanical properties of carbon nanotube/composites. In their investigation the stiffness of the epoxy matrix was controlled by changing the mixture ratio between the epoxy and hardener. Three-Point-Bending and Shore's hardness tests were conducted to determine the Young's modulus and hardness of the composites, respectively. Experimental data showed that the reinforcement role of the multi-walled carbon nanotubes decreased while increasing the stiffness matrix. Ci and Bai in [26] also found the same effect. In this last paper the effect of the epoxy matrix stiffness to the reinforcement role of CNTs was evaluated by controlling the curing process. They found that in the soft and ductile composites, carbon nanotubes provide a significant reinforcement without decreasing the fracture strain. Instead, the interface interaction between carbon nanotubes and matrix resulted poor in the stiff composite and therefore, they observed little contribution to the improvement in the mechanical properties of the composites.

In the present case we introduce very small carbon nanotube quantity (up to 0.6% in volume) in a very rigid composite with high modulus values, high glass transition temperature (236 °C); therefore we do not really expect a large improvement of either modulus or T_g. It is worth noting that our results on epoxy matrix can not be generalized. In fact, to evaluate the nanofiller reinforcement effect, Coleman et al. quantified the reinforcement as the rate of increase in modulus with respect to CNT volume fraction, dY/dV_f. They observed a slightly lower reinforcement value of dY/dV_f for blend composites of PA-6, acrylonitrile butadiene styrene (ABS) and CNTs with respect to rigid plastics [27].

In Fig. 8a and b dynamic mechanical curves of the resin with increasing concentrations of functionalized CNT are reported. Carbon nanotubes functionalized with –COOH show a different behavior respect to the previous. The presence and the increase of nanotube concentration does not determine an evident increase of the modulus, but an almost constant or even decreasing value of this parameter in the entire temperature range investigated. Also the glass transition shows a decrease of temperature for this system.

In addition, the samples with carbon nanotubes modified with –COOH groups, show two peaks in the tanδ indicating the presence of a lower temperature glass transition, beside the main transition at the same temperature as the pristine resin. The presence of a secondary peak, active at a lower temperature, in the loss factor suggests the presence of a fraction of amorphous phase with higher mobility due to a different degree of crosslinking. The position and the height of this secondary peak are depending on the nanotube concentrations. It can be again suggested that the presence of the –COOH groups catalyses either a fraction of homo-polymerization, or an esterification reaction, as hypothesized by the DSC curves, giving an interphase with a lower glass transition temperature, although regarding a phase nearer to the nanotubes. In other words the –COOH of the functionalized nanotubes can induce the formation of a more mobile phase around the nanotubes. This phase, having a lower glass transition temperature, as shown in Fig. 8b, and a lower modulus (as shown for a homopolymerized resin [22]) than the crosslinked resin, will hide the contribution of the stiffer carbon nanotubes, determining the lack of increase of the elastic modulus in the entire temperature interval. However, it is worth noting that on increasing the temperature, that means on going toward the lower glass transition (Fig. 8b) this effect is more evident, and the composite modulus is even more decreased. The effect of the –COOH modification is well evident in Fig. 9a and b, where a comparison between the neat resin and the composites with 1% of the two different carbon nanotubes is reported.

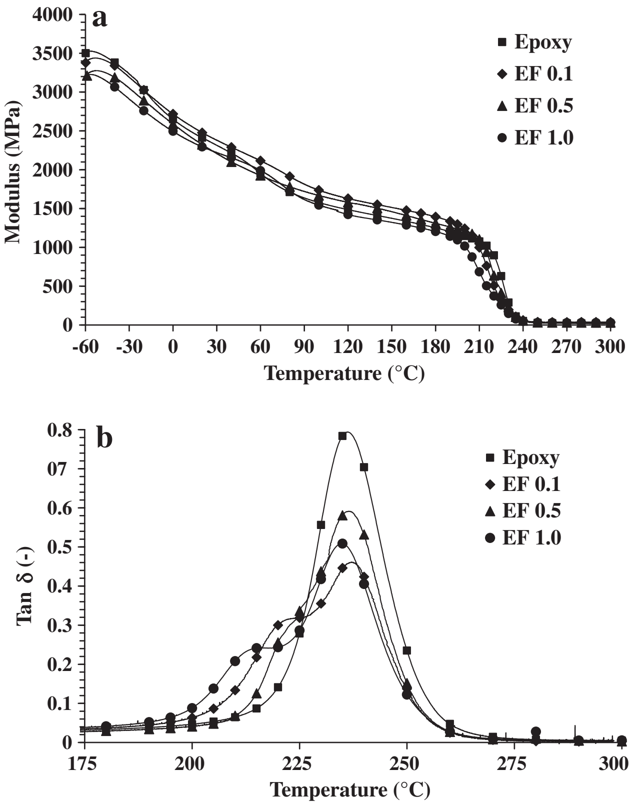

Fig. 8 – (a) Storage modulus, E′ (MPa) and (b) Loss factor (tanδ) of the pure epoxy and its composites with different MWCNT–COOH concentrations.

It is evident that the –COOH modification shows strong effect at low temperatures and in the proximity of the primary glass transition. In the range between 30 and 180 °C the elastic modulus of the pristine and MWCNT–COOH modified resin are very close. On the contrary, the resin modified with

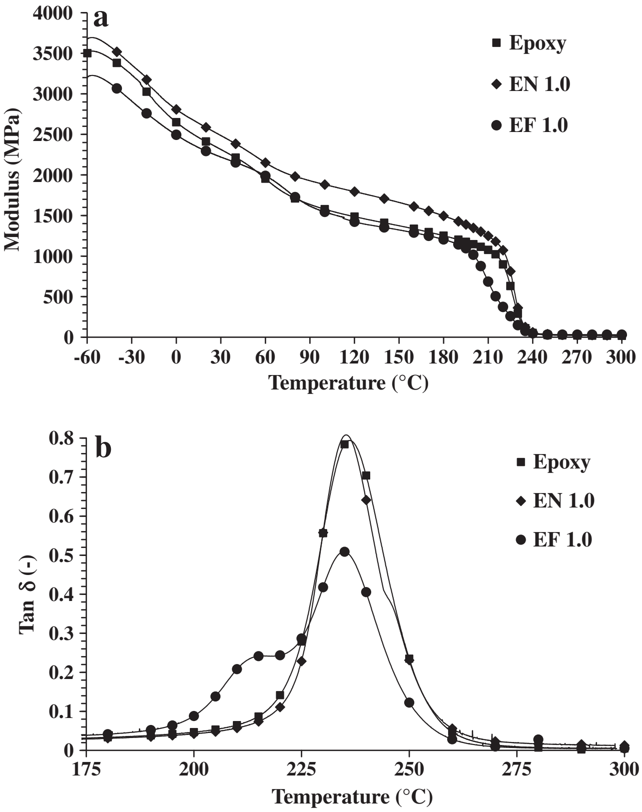

Fig. 9 – (a) Storage modulus, *E* (MPa) and (b) loss factor of the pure epoxy and its composites with 1 wt% of different MWCNTs.

Table 2 – Sorption values at equilibrium of liquid water into the three samples: Epoxy, resin with 0.5% of MWCNTs (EN) and resin with 0.5% of MWCNT-COOH (EF).

Sample	C_{eq}
Epoxy	4.03
EF 0.5	4.05
EF 0.5	4.02

MWCNTs shows a higher elastic modulus in all the temperature range. It is also evident the anticipation of the glass transition for the functionalized CNT, due to the presence of a second peak at lower temperature.

In conclusion, the functionalized nanotubes have no improvements on MWCNT/epoxy composite stiffness. In this case we even observe a decrease in the storage modulus with respect to the un-functionalized nanotubes. The lowest values observed for functionalized nanotubes are due to a reduction of the stiffness and strength of functionalized nanotubes, but very probably the decrease is mainly due to the presence of a fraction with a lower storage modulus.

3.2.5. Water transport properties

The transport properties, sorption and diffusion of a gas or a liquid into a polymeric matrix, can give interesting information about the amorphous phase of the system. Sorption is related to the thermodynamic interaction between the amorphous phase and the penetrating molecules, whereas diffusion, that is the kinetics of molecule transport, is mainly dependent on the free volume and can be decreased by the presence of impermeable obstacles, if these are able to increase the travelling molecule path. For example, in the case of semicrystalline polymers, it was found that the presence of the impermeable crystals becomes effective in reducing the diffusion parameter only for crystallinity higher than a critical value, also depending on the morphology [28]. Therefore we performed measurements of sorption and diffusion of liquid water at 25 °C for the neat resin, the resin with 0.5% of MWCNTs, and the resin with 0.5% of MWCNT–COOH. In Table 2 we report the sorption at equilibrium of liquid water into the three samples.

As expected, at high water activity no essential differences are evaluated between the samples, concerning the maximum water concentration at equilibrium. The thermodynamic interaction of the amorphous resin with liquid water is not changed by the presence of the carbon nanotubes. The resin is highly plasticized and the most part of water molecules form clusters inside the network. It is worth recalling that, in liquid water, at activity $a = 1$, the plasticizing effect is in the highest degree and hides differences that could be evaluated at lower activity of water. Indeed different behavior was observed for a resin filled with CNT at low water vapor activity [22]. In that case, at vapour activities between 0.2 and 0.6, both sorption and diffusion in the composites were found lower than in the pristine resin. The results of the present paper cannot be compared to the previous also because in the previous case the resin was cured with a tertiary amine, mainly giving a homopolymer, having a different interaction with water. In the present case we hypothesized a small fraction of homopolymer induced by the –COOH of the functionalized carbon nanotubes, and are interested to determine the diffusion behavior of the different samples.

In Fig. 10a the reduced curves, C_t/C_{eq}, as a function of square root of time, normalized for the thickness d of both the neat resin and the resin with 0.5% MWCNT are reported. We observe a Fickian behavior, that is a linear dependence of the reduced sorption on square root of time, a curvature for $C_t/C_{eq} > 0.8$ and a constant value at equilibrium. This Fickian behavior gives the possibility to derive the diffusion parameter, D (cm^2/s) by the first linear part of the curve, by the Eq. (1).

The concentration of water adsorbed at 25 °C, is reported as a function of time for the samples with 0.5 w% of MWCNTs (EN0.5) and with 0.5 w% of MWCNT–COOH (EF0.5), having the same thickness.

$$C_t/C_{eq} = 4/d\sqrt{D}t/\pi \tag{1}$$

where C_{eq} is the equilibrium concentration of water, C_t the concentration at time t, d (cm) is the thickness of the sample, and D (cm^2/s) the mean diffusion coefficient. The value of D results 2×10^{-9} cm^2/s.

In Fig. 10b we show the reduced curve for the composite sample with 0.5% of MWCNT–COOH. It is evident that the diffusion of water molecules into the composite sample with functionalized nanotubes, follows two curves. The first part, extending up to $C_t/C_{eq} = 0.7$, is coincident with the previous curves of neat epoxy and epoxy with 0.5% MWCNT, giving

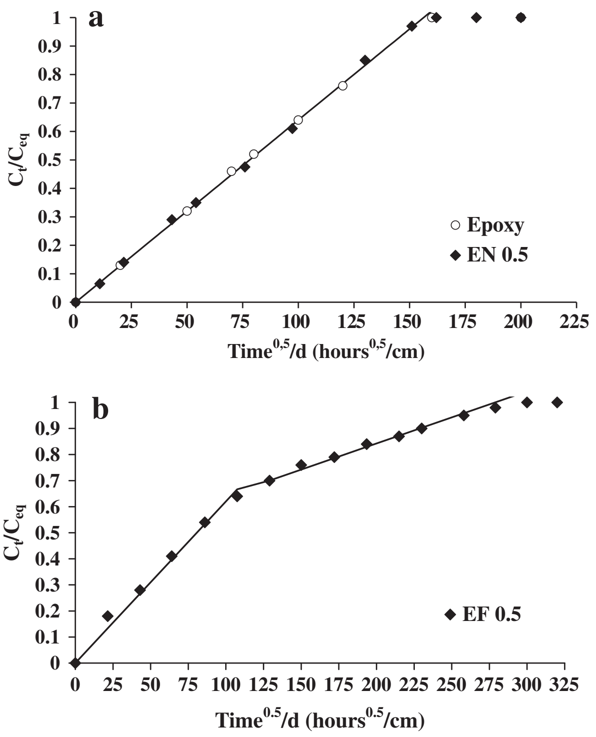

Fig. 10 – (a) C_t/C_{eq} against the square root of time of the neat resin and resin with 0.5% MWCNTs and (b) and the resin with 0.5% MWCNT–COOH.

the same angular coefficient. However a second stage appears, slowing down the diffusion process, allowing to reach the equilibrium value at longer times. This is due to the fraction of resin nearer to carbon nanotubes that contain impermeable obstacles more strictly adhering and therefore able to slow down the process in the final stage. This is a clear indication of a second phase, reasonably correspondent to the polymer forming a layer around the carbon nanotubes and therefore experiencing a different environment.

In any case the small peak in the dynamic DSC, the double peak in tanδ and the double behavior in the reduced sorption curve, all firmly point to the presence of two phases in the resin with –COOH-functionalized carbon nanotubes.

3.2.6. *Electrical conductivity*

The electrical conductivity of mixtures of CNTs (either SW or MW) and polymers is a widely investigated subject [8–17,29–33]. The conduction in CNTs composites has been explained by considering that conductive paths, causing the material to convert from an insulator to a conductor, are formed in the composite when the CNT concentration Φ increases over a threshold value Φ_c. The percolation theory describes the dependence of the conductivity σ on the filler concentration by a scaling law of the form $\sigma = \sigma_0 \cdot (\Phi - \Phi_c)^t$, where Φ_c is the percolation threshold and t an exponent depending on the system dimensionality [10–17,34–37]. In particular, in Ref. [37], on the basis of a comprehensive survey of the data available in the literature, some general results concerning a systematic correlation between material characteristics (polymeric matrices, CNT type, synthesis method, treatment, etc.) and parameters describing the percolation law are presented. Indeed, also the conductivity of our composites has been described in terms of percolation [17], but in this work we have chosen to focus our attention on the physical origins of the differences in the electrical conductivity and on the possibility to estimate some material characteristics for the systems under analysis which, in turn, may explain the differences obtained in the other measured physical properties.

At the onset of percolation, the charge transport follows a thermal fluctuation induced tunneling mechanism, in which the electrons through the thermally induced fluctuating potential barrier formed by a thin insulating polymer layer separating MWCNTs aggregates. However, a complete understanding of the relations among electrical properties, physical and chemical characteristics of the composite components (especially those pertaining to the interface between matrix and conducting inclusions) and the topological structures is still to be achieved. Therefore, additional efforts aimed at providing further information on the dependencies among electrical characteristics and the above mentioned parameters seems valuable.

Before analysing the electrical characteristics of the obtained composites, it is worth reminding that the structural properties of functionalized and non functionalized carbon nanotubes (average length, aspect ratio, etc.) are similar. Moreover, we have checked the "intrinsic" transport properties of the two types CNTs. We have verified that the conductivity of dense films of CNTs is $\geqslant 10^3$ S/m in both types. So, the small differences in the quantity of structural defects evidenced by the small discrepancy in the *R* value, obtained by the Raman spectra illustrated in par. 3.1.2 do not affect the "intrinsic" conductivity of the two types of CNTs.

On the basis of the above observations, if the conductivity of the composites obey to simple mixing models taking into account only the electrical properties of the different components and their concentration, one expects that the conductivity of two examined composites should evidence similar behaviors, i.e. comparable equivalent conductivity for same CNTs loadings. Moreover, the conductivity at high CNT concentrations is supposed to reach a limit value which cannot be higher than that measured for the dense films.

The behavior of the static volume conductivity of MWCNTs and functionalized MWCNTs vs. the filler concentration at room temperature is summarized in Figs. 11 and 12. Some remarkable differences can be evidenced from such plots. As shown in Fig. 11, the EN composites exhibit the typical abrupt increase of the conductivity from the value of the pure epoxy resin (3.3×10^{-15} S/m) to a very high one (7.5×10^{-3} S/m) predicted by the percolation theory with a $\Phi_c \leqslant 0.1\%$. By increasing the MWCNT percentage up to 1%, a high value of conductivity (4.3×10^{-1} S/m) is achieved. The conductivity does not reach the values obtained for dense films at the explored concentrations levels of CNTs ($\sim 10^3$ S/m) owing to the effect of nanotube/nanotube contact resistance described in [38]. In their studies on the role of tunnelling resistance in the electrical conductivity of carbon nanotube-based composites, Li et al. [38] using Monte Carlo simulations found that the tunnelling resistance plays a dominant role in the electrical conductivity of composites.

The conductivity of our EF composites shows a much broader transition from figures comparable to that of the

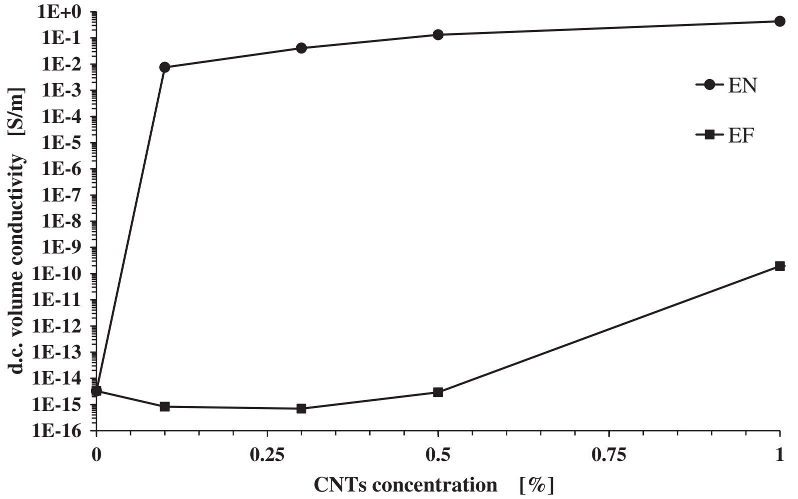

Fig. 11 – Dc volume conductivity vs. CNTs concentration for nonfunctionalized (EN) and COOH-functionalized CNT (EF) composites.

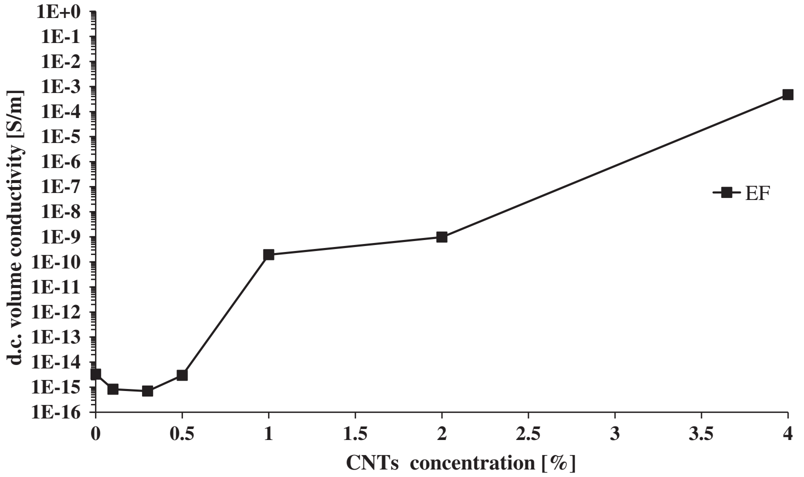

Fig. 12 – Dc volume conductivity vs. CNTs concentration for COOH-functionalized CNT (EF) composites.

insulating matrix to values typical of a conductive structure, as evidenced by the bottom curve of Figs. 11 and 12. It can be noted that the percolation threshold happens around 0.5% of functionalized MWCNTs and that for Φ between 1% and 2% the conductivity still exhibits a limited increase (if compared to that of the EN systems) with a value of 1.9×10^{-10} S/m. A significant increase is obtained, as shown in Fig. 12, only at 4% of functionalized MWCNTs. Samples with values of concentration higher than 4% have not been arranged due to the difficulties associated to the very high viscosity of the composites hindering the preparation procedure.

The obtained limit value of the conductivity for the EF systems (4.7×10^{-4} S/m) is in any case about three orders of magnitude lower than that measured for the EN composites. Since the intrinsic properties of the basic components of the composites are the same and also the dispersion levels of the two types of CNTs are comparable in both systems, as evidenced in par. 3.2.2, such unlike behavior has to be ascribed to other phenomena. In particular, according to the model proposed in Ref. [38], a variable tunneling (contact) resistance between nanotubes due to insulating wrappings (sheaths) of different thickness may be considered to explain the observed differences. The tunneling resistance, which is calculated by assuming a rectangular potential barrier, depends only weakly on the CNT intrinsic conductivity and tube diameter, whereas the thickness of the sheaths induces an exponential increase. Although such a model refers to simple configurations with perpendicular intersections between nanotubes in a layer (complex structures due to CNT agglomeration are not taken into account), nevertheless it can be used to estimate, in an “average” sense, some characteristics of the systems under analysis.

Furthermore, percolation thresholds below 0.1% are usually attributed to kinetic percolation which allows for filler movement and re-aggregation [37]. Sheathing effect results in a higher percolation threshold both for the reduced movement of wrapped CNTs and for the obviously suppressed formation of conductive paths.

In particular, for a 1% concentration of CNTs a difference of about nine order of magnitude between the two composites conductivity can be noted which can be attributed to a like variation in the tunnelling resistance. The simulation results presented in Ref. [38] show that a conductivity of about 0.1 S/m, like that one measured for the EN composites at 1% loading, can be achieved, for the same CNTs concentration, by considering a tunneling contact resistance of $10^8\,\Omega$. This value of resistance corresponds to a thickness of the insulating layer (in the case of CNTs with a diameter of 10 nm inside an epoxy matrix) of about 0.7 nm. In order to get a nine order of magnitude increase (like that corresponding to the increment of the EF system resistivity with respect to that of the EN composites at 1% CNT loading) in the contact resistance, the thickness of the insulating layer has to be equal to about 1.6 nm. Moreover, in order to achieve the conductivity values (4.7×10^{-4} S/m) obtained for the composites with the highest concentration (4%) of functionalized CNTs, a contact resistance of about $10^{10}\,\Omega$ has to be accounted for which, in turn, corresponds to an insulating layer thickness of about 0.9 nm.

Such theoretically argued differences in the thickness of the insulating layer around CNTs are also consistent with the observations that, differently from the EN composites, the EF systems show a more appreciable residue of epoxy resin between nanotubes (even after the etching attack) probably due to the ability of the COOH groups to create stronger adhesion with the polymeric matrix. This conjecture is also in accordance with the observed differences in the diffusion properties.

4. Conclusions

In this paper the mechanical and electrical properties of epoxy composite systems loaded with increasing concentration of multi-walled and chemically functionalized carbon nanotubes have been discussed with reference to the morphological characteristics of the composites.

A careful observation by SEM highlights for both the samples with MWCNTs and MWCNT–COOH (EN0.5 and EF0.5) a homogeneous structure in which CNTs are uniformly distributed in a close net through the epoxy matrix. However the etching procedure is more efficient for composites filled with un-functionalized MWCNTs whereas in the resin with functionalized ones nanotubes strong interconnections between nanotubes and residual polymeric matrix remain after the etching attack, indicating a more connected phase. The addition of 1.0% of carbon nanotubes determines an improvement of the storage modulus of about 20% for the NF based composites, whereas for the CNTs– functionalized with –COOH the concentration increase does not determine an increase of the elastic modulus in the entire temperature range investigated. Also the glass transition shows a decrease for this system. This behavior can be attributed to the fact that the presence of the –COOH groups catalyses a fraction of homo-polymerization, having a lower glass transition temperature. This could also explain the almost constant elastic modulus in the entire temperature interval. Both dynamic mechanical analysis and transport properties of liquid water indicate the presence of two phases in the resin with functionalized CNT. This was attributed to a fraction of homo-polymerization induced by the –COOH on the nanotubes. The presence of this phase more adherent to the nanotubes determines a higher tunneling resistance between interacting CNTs and therefore a higher percolation threshold and lower limit value of the conductivity.

Acknowledgements

The authors wish to thank Raffaele Raimo for the assistance in performing the electrical measurements. This work has been partly supported by the Italian Ministry for Education, University and Research (MIUR) within the National Project PRIN 2008NMRHJS “Development and Electromagnetic Characterization of Nano Structured Carbon Based Polymer Composites (DENSE)” and FARB funds of the University of Salerno.

Appendix A. Supplementary data

Supplementary data associated with this article can be found, in the online version, at doi:10.1016/j.carbon.2011.01.017.

REFERENCES

[1] Iijima S. Helical microtubules of graphitic carbon. Nature 1991;354(6348):56–8.

[2] Ajayan PM, Zhou OZ. Applications of carbon nanotubes. In: Dresselhaus MS, Dresselhaus G, Avouris Ph, editors. Carbon nanotubes: synthesis, structure, properties and applications, vol 80. Berlin: Springer; 2001. p. 391–425.

[3] Saito R, Dresselhaus G, Dresselhaus MS. Physical properties of carbon nanotubes. London: Imperial College Press; 1998.

[4] Coleman JN, Khan U, Blau WJ, Gun’ko YK. Small but strong: a review of the mechanical properties of carbon nanotube–polymer composites. Carbon 2006;44(9):1624–52.

[5] Xie XL, Mai YW, Zhou XP. Dispersion and alignment of carbon nanotubes in polymer matrix: a review. Mate Sci Eng R: Rep 2005;49(4):89–112.

[6] Ounaies Z, Park C, Wise KE, Siochi EJ, Harrison JS. Electrical properties of single wall carbon nanotube reinforced polyimide composites. Compos Sci Technol 2003;63(11):1637–46.

[7] Thostenson ET, Ren Z, Chou TW. Advances in the science and technology of carbon nanotubes and their composites: a review. Compos Sci Technol 2001;61(13):1899–912.

[8] Sandler J, Shaffer MSP, Prasse T, Bauhofer W, Schulte K, Windle AH. Development of a dispersion process for carbon nanotubes in an epoxy matrix and the resulting electrical properties. Polymer 1999;40(21):5967–71.

[9] Song YS, Youn JR. Influence of dispersion states of carbon nanotubes on physical properties of epoxy nanocomposites. Carbon 2005;43(7):1378–85.

[10] Martin CA, Sandler JKW, Windle AH, Schwarz MK, Bauhofer W, Schulte K, et al. Electric field-induced aligned multi-wall carbon nanotube networks in epoxy composites. Polymer 2005;46(3):877–86.

[11] Sandler JKW, Kirk JE, Kinloch IA, Shaffer MSP, Windle AH. Ultra-low electrical percolation threshold in carbon-nanotube–epoxy composites. Polymer 2003;44(19):5893–9.

[12] Moisala A, Li Q, Kinloch IA, Windle AH. Thermal and electrical conductivity of single- and multi-walled carbon nanotube–epoxy composites. Compos Sci Technol 2006;66(10):1285–8.

[13] Kovacs JZ, Velagala BS, Schulte K, Bauhofer W. Two percolation thresholds in carbon nanotube epoxy composites. Compos Sci Technol 2007;67(5):922–8.

[14] Kim YJ, Shin TS, Choi HD, Kwon JH, Chung YC, Yoon HG. Electrical conductivity of chemically modified multiwalled carbon nanotube/epoxy composites. Carbon 2005;43(1):23–30.

[15] Du F, Fischer JE, Winey KI. Effect of nanotube alignment on percolation conductivity in carbon nanotube/polymer composites. Phys. Rev. B 2005;72(12):121404-1, 4.

[16] Spitalsky Z, Krontiras CA, Georga SN, Galiotis C. Effect of oxidation treatment of multiwalled carbon nanotubes on the mechanical and electrical properties of their epoxy composites. Compos Part A 2009;40(6–7):778–83.

[17] Guadagno L, Naddeo C, Vittoria V, Sorrentino A, Vertuccio L, Raimondo M, et al. Cure behavior and physical properties of epoxy resin—filled with multiwalled carbon nanotubes. J Nanosci Nanotechnol 2010;10(4):2686–93.

[18] Dresselhaus MS, Dresselhaus G, Saito R, Jorio A. Raman spectroscopy of carbon nanotubes. Phys Rep 2005;409:47–99.

[19] Liu Y, Vander Wal RL, Khabashesku VN. Functionalization of carbon nano-onions by direct fluorination. Chem Mater 2007;19(4):778–86.

[20] Osswald S, Havel M, Gogotsi Y. Monitoring oxidation of multiwalled carbon nanotubes by Raman spectroscopy. J Raman Spectrosc 2007;38(6):728–36.

[21] Costa S, Borowiak-Palen E, Kruszynska M, Bachmatiuk A, Kalenczuk RJ. Characterization of carbon nanotubes by Raman spectroscopy. Mater Sci (Poland) 2008;26(2):433–41.

[22] Guadagno L, Vertuccio L, Sorrentino A, Raimondo M, Naddeo C, Vittoria V, et al. Mechanical and barrier properties of epoxy resin filled with multi-walled carbon nanotubes. Carbon 2009;47(10):2419–30.

[23] Zhou YX, Wu PX, Cheng ZY, Ingram J, Jeelani S. Improvement in electrical, thermal and mechanical properties of epoxy by filling carbon nanotube. Express Polym Lett 2008;2(1):40–8.

[24] Zhou Y, Pervin F, Lewis L, Jeelani S. Experimental study on the thermal and mechanical properties of multi-walled carbon nanotube-reinforced epoxy. Mater Sci Eng A 2007;452–453:657–64.

[25] Her S, Yeh S. Influence of multi-walled carbon nanotubes on the mechanical properties of nanocomposites. Adv Mater Res 2010;139–141:9–12.

[26] Ci L, Bai J. The reinforcement role of carbon nanotubes in epoxy composites with different matrix stiffness. Compos Sci Technol 2006;66:599–603.

[27] Coleman JN, Khan U, Gun'ko YK. Mechanical reinforcement of polymers using carbon nanotubes. Adv Mater 2006;18:689–706.

[28] D'Aniello C, Guadagno L, Gorrasi G, Vittoria V. Influence of the crystallinity on the trasport properties of isotactic polypropylene. Polymer 2000;41(7):2515–9.

[29] Bryning MB, Islam MF, Kikkawa JM, Yodh AG. Very low conductivity threshold in bulk isotropic single-walled carbon nanotube-epoxy composites. Adv Mater 2005;17(9):1186–91.

[30] Vionnet-Menot S, Grimaldi C, Maeder T, Strässler S, Ryser P. Tunneling-percolation origin of nonuniversality: theory and experiments. Phys. Rev. B 2005;71(6):064201–64212.

[31] Mdarhri A, Carmona F, Brosseau C, Delhaes P. Direct current electrical and microwave properties of polymer-multiwalled carbon nanotubes composites. J Appl Phys 2008;103(5):054303–54309.

[32] Barrau S, Demont P, Peigney A, Laurent C, Lacabanne C. DC and AC conductivity of carbon nanotubes-polyepoxy composites. Macromolecules 2003;36(4):5187–94.

[33] Jonscher AK. The 'universal' dielectric response. Nature 1977;267(5613):673–9.

[34] Kimakis E, Amaratunga GAJ. Electrical properties of single wall carbon nanotube–polymer composite films. J Appl Phys 2006;99:084302-1, 7.

[35] Gorrasi G, Sarno M, Di Bartolomeo A, Sannino D, Ciambelli P, Vittoria V. Incorporation of carbon nanotubes into polyethylene by high energy ball milling: morphology and physical properties. J Polym Sci Part B: Polym Phys 2007;45:597–606.

[36] De Vivo B, Guadagno L, Lamberti P, Raimo R, Sarto MS, Tamburrano, Tucci V, et al. Electromagnetic properties of carbon nanotube/epoxy nanocomposites. In: International Symposium on electromagnetic compatibility – EMC Europe 2009, 11–12 June 2009. p. 1–4, doi:10.1109/EMCEUROPE.2009.5189674.

[37] Bauhofer W, Kovacs JZ. A review and analysis of electrical percolation in carbon nanotubes polymer composites. Compos Sci Technol 2009;69:1486–98.

[38] Li C, Thostenson ET, Chou TW. Dominant role of tunneling resistance in the electrical conductivity of carbon nanotube-based composites. Appl Phys Lett 2007;91(22):223114-1, 3.